

ELMM: Efficient Lightweight Multimodal Large Language Models for Multimodal Knowledge Graph Completion

Wei Huang¹, Peining Li¹, Meiyu Liang¹, Xu Hou¹, Junping DU¹, Yingxia Shao¹, Guanhua Ye¹,
Wu Liu¹, KangKang Lu¹, Yang Yu¹

¹School of Computer Science, Beijing University of Posts and Telecommunications,

Abstract

Multimodal Knowledge Graphs (MKGs) extend traditional knowledge graphs by incorporating visual and textual modalities, enabling richer and more expressive entity representations. However, existing MKGs often suffer from incompleteness, which hinders their effectiveness in downstream tasks. Therefore, multimodal knowledge graph completion (MKGC) task is receiving increasing attention. While large language models (LLMs) have shown promise for knowledge graph completion (KGC), their application to the multimodal setting remains underexplored. Moreover, applying Multimodal Large Language Models (MLLMs) to the task of MKGC introduces significant challenges: (1) the large number of image tokens per entity leads to semantic noise and modality conflicts, and (2) the high computational cost of processing large token inputs. To address these issues, we propose Efficient Lightweight Multimodal Large Language Models (**ELMM**) for MKGC. ELMM proposes a Multi-view Visual Token Compressor (**MVTC**) based on multi-head attention mechanism, which adaptively compresses image tokens from both textual and visual views, thereby effectively reducing redundancy while retaining necessary information and avoiding modality conflicts. Additionally, we propose an attention pruning strategy to remove redundant attention layers in MLLMs, substantially reducing inference cost. To mitigate the performance degradation introduced by pruning, we further incorporate a linear projection for error compensation. Extensive experiments on four benchmark datasets demonstrate that ELMM achieves state-of-the-art performance.

1 Introduction

Knowledge Graphs (KGs) represent real-world knowledge in a structured form using factual triples (head, relation, tail). In recent years, they have attracted considerable attention from both academia

and industry, and have been widely applied to various downstream tasks such as information retrieval (Yang, 2020; Wang et al., 2024), and recommendation systems (Guo et al., 2020; Jiang et al., 2024). Multimodal Knowledge Graphs (MKGs) enhance traditional KGs by integrating information from multiple modalities, such as text and images, thereby enabling richer and more accurate knowledge representations. This multimodal fusion has shown to improve the performance of a wide range of intelligent systems (Guo et al., 2024b). However, existing MKGs often suffer from incomplete information, which limits their effectiveness in practical applications. To address this challenge, the task of Multimodal Knowledge Graph Completion (MKGC) has emerged and has seen rapid development (Gao et al., 2025a; Zhang et al., 2024a; Chen et al., 2022; Shang et al., 2024). The core objective of MKGC is to leverage multimodal data to enhance the expressiveness of entity representations and uncover latent knowledge, thereby completing missing information in MKGs.

Large models, through extensive pre- and post-training on massive datasets, exhibit emergent capabilities and encode rich real-world knowledge (Guo et al., 2025a; Xiong et al., 2025), making them promising for KGC. For example, KICGPT (Wei et al., 2024) addresses the long-tail issue by re-ranking candidate triples from traditional methods, while MKGL (Guo et al., 2024a) investigates whether LLMs can comprehend the structured representation of knowledge in the form of triples (head, relation, tail). However, current research largely overlooks multimodal inputs, leaving the potential of multimodal large language models (MLLMs) for MKGC underexplored.

In MKGs, entities are typically associated with various modalities of information, such as images and textual descriptions. For example, in datasets like FB15k-237-IMG (Bollacker et al., 2008) and WN18-IMG (Bordes et al., 2013), each entity is

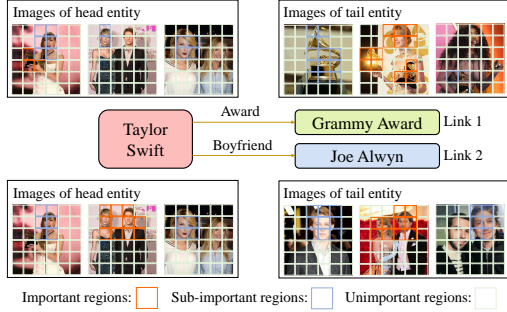


Figure 1: A description of each associated image region’s contribution to the entity Taylor Swift in a different link.

linked to 10 images along with corresponding textual descriptions, providing rich multimodal contextual information to complement the structured triples. State-of-the-art MLLMs (e.g., LLaVA-1.5 (Liu et al., 2024), Qwen2.5-VL (Bai et al., 2025), and MobileVLM (Chu et al., 2023)) typically employ visual encoders, such as ViT (Dosovitskiy et al., 2020), to encode different regions of an image into a sequence of image tokens. These image tokens are then concatenated with text tokens and jointly processed by MLLMs in a unified framework. However, directly applying existing multimodal fusion paradigms to MKGC poses several challenges. First, **the number of image tokens per entity is large and often redundant**. Standard visual encoders generate hundreds of tokens per image; with 10 images per entity, this results in thousands of tokens. Moreover, the semantic relevance of visual regions is relation-dependent: as illustrated in Figure 1, different relations emphasize different regions of Taylor Swift. Naively concatenating all visual and textual tokens therefore introduces noise and cross-modal interference, impeding effective semantic alignment. Second, **the computational cost of processing such large token inputs is prohibitive**. In MLLMs, the computational complexity of attention mechanisms typically grows quadratically with the number of tokens, while memory consumption increases at least linearly. This limits the model’s applicability in large-scale MKGC scenarios.

To address the above challenges, we propose ELMM, the first novel method to leverage **Efficient Lightweight Multimodal Large Language Models (ELMM)** for MKGC. First, we propose a **Multi-view Visual Token Compressor (MVTC)** based on multi-head attention to select the most informative visual tokens from both textual and visual

views. MVTC adaptively compresses visual tokens according to their semantic relevance to the textual description (entities and relations) and their intrinsic visual salience, aggregating tokens from multiple images into a fixed set of high-information representations. This design effectively reduces visual noise and modality interference, improving both inference efficiency and representational capacity. Second, we empirically identify structural redundancy in MLLM attention layers for MKGC, where certain layers produce highly similar input–output representations and contribute marginally to performance. To address this, we propose an attention pruning strategy that removes such redundant layers, significantly reducing inference overhead. We further observe that the pruning-induced error can be effectively compensated by a linear projection, and accordingly design a principled initialization pipeline for this projection.

Our contributions can be summarised as follows:

- We propose **Efficient Lightweight Multimodal Large Language Models (ELMM)** for multimodal knowledge graph completion, a novel MKGC method that designs a **Multi-view Visual Token Compressor (MVTC)** based on multi-head attention mechanism to adaptively compress image tokens from both textual and visual views. This mechanism enables effective compression of multimodal inputs while mitigating modality conflicts and reducing noise. To the best of our knowledge, this is the first work to address the MKGC task using MLLMs.
- We propose an attention pruning strategy that identifies and removes redundant attention layers in MLLMs for the MKGC task, thereby reducing computational overhead. To mitigate pruning-induced errors, we apply linear projection as compensation.
- Extensive experiments on four benchmark datasets demonstrate the superiority of ELMM in the MKGC task.

2 Methodology

2.1 Preliminaries

2.1.1 Problem Formulation

A multimodal knowledge graph (MKG) is defined as a directed graph $MKG = (\mathcal{E}, \mathcal{R}, \mathcal{G}, \mathcal{A}_M)$,

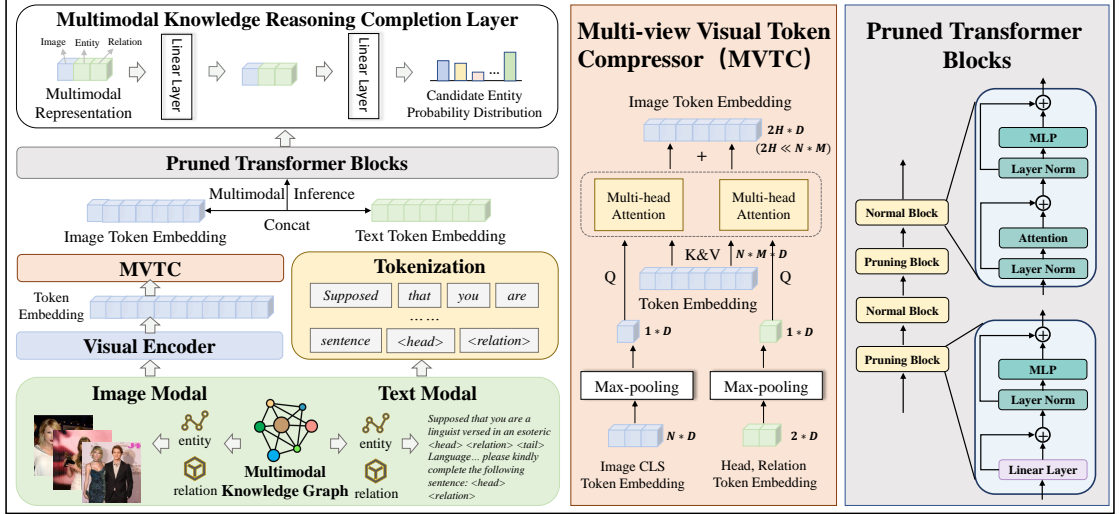


Figure 2: Overview of the ELMM architecture. From left to right: (1) ELMM processes input text and images containing incomplete triplet information; (2) MVTC adaptively compresses image tokens from both textual and visual views; (3) MLLM attention pruning and compensation mechanism.

where \mathcal{E} and \mathcal{R} denote the sets of entities and relations, respectively. The factual triples are represented as $\mathcal{G} = \{(e_h, r_{h,t}, e_t) \mid e_h, e_t \in \mathcal{E}, r_{h,t} \in \mathcal{R}\}$. Each entity is associated with a set of multimodal attributes \mathcal{A}_M , which includes textual \mathcal{M}_t and visual \mathcal{M}_v modalities. The task of multimodal knowledge graph completion (MKGC) aims to infer missing entities in \mathcal{G} . Given an incomplete triple $(h, r, ?)$ or $(?, r, t)$, the goal is to predict the missing entity t or h .

2.1.2 Multimodal Large Language Models

Generally, a multimodal large language model comprises the following components: a visual encoder and a textual tokenizer, which respectively segment images into multiple regions and encode it into a sequence of image token embeddings $I_{temp} \in \mathbb{R}^{NM \times E_i}$ (N represents the number of images, M represents the region of each image, and E_i represents the dimension), while simultaneously converting the input text into a series of text token embeddings $T_t \in \mathbb{R}^{K \times D}$ (K is the number of text tokens and D is the dimension). The image token embeddings are then projected into the same dimensional space as the text embeddings via a linear transformation, yielding $I_t \in \mathbb{R}^{NM \times D}$. These are concatenated with the text embeddings to form a unified multimodal token sequence $T \in \mathbb{R}^{(NM+K) \times D}$; A series of transformer blocks \mathcal{M} , which processes the multimodal token sequence and generates a corresponding sequence of hidden states for prediction;

tion;

$$\mathbf{h}_{0:NM+K-1}^m = \mathcal{M}(t_{0:NM+K-1}) \quad (1)$$

and a head layer, which maps each hidden state to a probability distribution $\mathbf{p}_n = \text{head}(\mathbf{h}_{NM+K}^m)$.

2.2 ELMM Framework

The overall architecture of ELMM is depicted in Figure 2. Applying conventional multimodal large language models (MLLMs) directly to MKGC generates excessive image tokens (e.g., over 1,000 tokens from 10 entity-related images after encoding), introducing noise and exacerbating modality conflicts. To mitigate these issues, ELMM proposes a **Multi-view Visual Token Compressor (MVTC)** based on multi-head attention mechanism, which leverages multi-head attention to adaptively compress image tokens from both textual and visual views. MVTC effectively retains text-relevant information and key image details, thereby facilitating robust cross-modal alignment. Moreover, during MKGC, certain attention layers within the transformer blocks \mathcal{M} exhibit high input-output similarity, indicating computational redundancy. ELMM addresses this by incorporating an **attention pruning strategy** that eliminates such redundant layers. A linear compensation module is then employed to mitigate approximation errors introduced by pruning, resulting in the pruned transformer blocks denoted as \mathcal{M}' . Finally, to better support MKGC, ELMM replaces the traditional head layer with a multimodal knowledge reasoning

completion layer, improving cross-modal fusion and generating a probability distribution over candidate entities.

2.3 Multi-view Visual Token Compressor

The overall workflow of **Multi-view Visual Token Compressor (MVTC)** is illustrated in the middle section of Figure 2. Considering that the importance of an image token can vary across different relational contexts (see Figure 1), MVTC first starts from the textual view and compresses image tokens using entity and relation tokens from text. This process retains the token representations that are most strongly associated with text information, thereby achieving modality alignment. Specifically, we concatenate the entity and relation token embeddings, denoted as T_{entity} and T_{relation} , respectively, and apply max-pooling to obtain a fused textual representation $X_t \in \mathbb{R}^{1 \times D}$. This representation X_t , together with the image token embeddings I_t , is used as input to a Multi-Head Attention (MHA) mechanism. The attention computation is defined as:

$$Q_i = X_t W_i^Q, K_i = I_t W_i^K, Q_i \in \mathbb{R}^{1 \times d}, K_i \in \mathbb{R}^{MN \times d} \quad (2)$$

$$V = I_t W^V, \quad V \in \mathbb{R}^{NM \times D} \quad (3)$$

$$\begin{aligned} \text{Head}_i &= \text{Attention}(Q_i, K_i, V) \\ &= \text{softmax}\left(\frac{Q_i K_i^T}{\sqrt{d}}\right) V, \quad \text{Head}_i \in \mathbb{R}^{1 \times D} \end{aligned} \quad (4)$$

$$I_{\text{text}} = \text{Concat}(\text{Head}_1, \dots, \text{Head}_H), I_{\text{text}} \in \mathbb{R}^{H \times D} \quad (5)$$

Here, W_i^Q, W_i^K, W^V are trainable projection matrices; d denotes the dimensionality of the queries and keys, where $d = D/H$, and H is the number of attention heads. The obtained I_{text} represents the result of compressing the image tokens from the textual view. Meanwhile, to ensure the effective preservation of core information in images, MVTC also performs compression on image tokens from the visual view. Specifically, to preserve the most representative global information from the images, we first extract the CLS tokens from multiple images and concatenate them to form:

$$T_{\text{CLS}} = \text{concat}(\text{CLS}_1, \text{CLS}_2, \dots, \text{CLS}_N). \quad (6)$$

We then apply a max-pooling operation over T_{CLS} to obtain a fused representation, denoted as X_i . Similar to the calculation process of I_{text} , we use

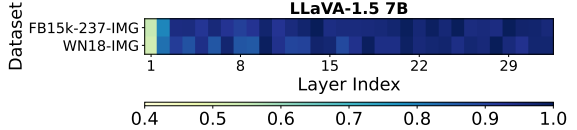


Figure 3: Cosine similarity between the input and output of the attention layer in the training data of FB15k-237-IMG and WN18-IMG. The calculation method is to take 1,000 data points from the training set, perform inference, and calculate the average cosine similarity.

X_i and I_T as the input of MHA to finally obtain I_{image} . The obtained I_{image} contains the most important information of the image itself, representing the visual token information compressed from the visual view. We concatenate I_{image} , I_{text} , and T_t to obtain T , and then reason through the pruned transformer blocks \mathcal{M}' to obtain hidden states $\mathbf{h}_{0:2H+K-1}^m$. As a result, the aggregated hidden states retain not only essential visual information but also visual cues semantically aligned with the textual modality.

2.4 Attention Pruning Strategy

Due to the high computational cost of attention mechanisms, they often introduce significant inference latency. For instance, with an input sequence length of 512 tokens, the attention module alone can introduce up to 0.3437 seconds of latency per inference, accounting for approximately 77.9% of the total inference time (0.4410 seconds). To mitigate this overhead, we perform a redundancy analysis of the attention modules in MLLMs, such as LLaVA-1.5 (Liu et al., 2024), during MKGC task. Specifically, we measure the cosine similarity between the input and output of each attention module to assess its redundancy. As illustrated in Figure 3, the upper layers of the model consistently exhibit high input-output similarity across various experimental settings. This observation suggests a significant degree of computational redundancy in certain attention modules of MLLMs during MKGC task.

Based on this finding, we propose an Attention Pruning Strategy that selects the top- K layers with the highest input-output cosine similarity and prunes their attention modules. However, the direct removal of attention mechanisms inevitably introduces a forward propagation error, denoted as $\varepsilon = x^{\text{ori}} - x^{\text{pruning}}$, where x^{ori} is the original output and x^{pruning} is the output after pruning. To compensate for the error we utilize a linear projec-

tion $x^{pruning}W_c$ to fit the error ε . Then, we propose a training-free initialization method for W_c . Furthermore, we provide the following theorem to guide the initialization of W_c :

Theorem 1. *The initialization of W_c that minimizes the expected compensation error satisfies:*

$$W_c = V\Sigma^+U^T\mathbb{E}(\varepsilon), \quad (7)$$

where $U\Sigma V^T$ is the SVD decomposition of $\mathbb{E}(x^{pruning})$, Σ^+ denotes the pseudoinverse of Σ .

Proof. Minimizing the expected compensation error corresponds to solving the following optimization problem:

$$\min_{W_c} \|\mathbb{E}[x^{pruning}]W_c - \mathbb{E}[\varepsilon]\|^2. \quad (8)$$

Since W_c is independent of the data distribution, the expectation operator can be applied to $x^{pruning}$ and ε separately. Thus, the problem reduces to:

$$\min_{W_c} \|\mathbb{E}[x^{pruning}]W_c - \mathbb{E}[\varepsilon]\|^2. \quad (9)$$

This is a standard least-squares problem with the solution:

$$W_c = \mathbb{E}[x^{pruning}]^+ \mathbb{E}[\varepsilon], \quad (10)$$

where $\mathbb{E}[x^{pruning}]^+$ is the Moore–Penrose pseudoinverse of $\mathbb{E}[x^{pruning}]$. Given the SVD $\mathbb{E}[x^{pruning}] = U\Sigma V^T$, the pseudoinverse is $\mathbb{E}[x^{pruning}]^+ = V\Sigma^+U^T$, leading to the final result:

$$W_c = V\Sigma^+U^T\mathbb{E}[\varepsilon]. \quad (11)$$

□

In practical applications, we randomly sampled 1,000 instances from the training dataset and employed the average values of $\bar{x}^{pruning}$ and $\bar{\varepsilon}$ as estimators for $\mathbb{E}(x^{pruning})$ and $\mathbb{E}(\varepsilon)$, respectively. Considering that errors in the early layers of the compensation model may propagate and affect the representations in subsequent layers, we adopted a bottom-up strategy to initialize W_c . Experimental results on the FB15k-237-IMG dataset demonstrate that, after applying linear compensation, the error of LLaVA-1.5 7B is significantly reduced from 276.5 (without compensation) to 4.7, corresponding to only 1.7% of the original error. This significant improvement underscores the effectiveness of our linear compensation method.

Dataset	#Rel.	#Ent.	#Train	#Dev	#Test
FB15k-237-IMG	237	14,541	272,115	17,535	20,466
WN18-IMG	18	40,943	141,442	5,000	5,000
DB15K	279	12842	79222	9902	9904
MKG-W	169	15000	34196	4276	4274

Table 1: Statistics of Dataset.

2.5 Multimodal Knowledge Reasoning Completion Layer

To fit the multimodal knowledge graph completion task, we employ a multimodal knowledge reasoning completion layer to compute the probability distribution over candidate entities. The process is defined as follows:

$$E_m = [E_{image}, E_{entity}, E_{relation}], S \in \mathbb{R}^{1 \times 3D} \quad (12)$$

$$E'_m = LinearLayer(E_m), E'_m \in \mathbb{R}^{1 \times 3D} \quad (13)$$

$$p = LinearLayer(E'_m), p \in \mathbb{R}^{1 \times r} \quad (14)$$

Here, E_{image} is obtained by max-pooling over the hidden states of image modality hidden states. E_{entity} and $E_{relation}$ correspond to the hidden states of the entity and relation tokens. These are concatenated to form the multimodal representation E_m . The fused representation is first processed by a linear layer and then projected to obtain the probability distribution $p \in \mathbb{R}^{1 \times r}$ of the candidate entities, where r represents the number of entities.

2.6 Optimization

To optimize ELMM, we employ a contrastive learning objective, defined as follows:

$$\begin{aligned} \mathcal{L} = & \sum_{(e_i, r_k, e_j) \in \mathcal{T}_{train}} \left[-\log(p_{e_j}) \right. \\ & \left. + \frac{1}{|\mathcal{N}_{neg}(e_j)|} \sum_{e_{neg} \in \mathcal{N}_{neg}(e_j)} \log(1 - p_{e_{neg}}) \right]. \end{aligned} \quad (15)$$

Here, $\mathcal{N}_{neg}(e_j) = \{e_{neg} \cup e_i \mid e_{neg} \neq e_j, e_{neg} \in \mathcal{E}\}$ denotes the set of negative samples for the target entity e_j . Since the prediction of tail entities in the form of $(e_i, r_k, ?)$ often results in a bias where the head entity e_i is assigned disproportionately high confidence, we incorporate a self-denoising strategy by treating the head entity e_i as a hard negative sample. The loss function \mathcal{L} is in a form of a binary cross-entropy.

Model Name	FB15k-237-IMG				WN18-IMG			
	MR	Hits@1	Hits@3	Hits@10	MR	Hits@1	Hits@3	Hits@10
Multi-modal KGC Models								
TransAE(IJCNN 2019)	431	19.9	31.7	46.3	352	32.3	83.5	93.4
RSME(ACMMM 2021)	417	24.2	34.4	46.7	223	94.3	95.1	95.7
KG-BERT(2019)	153	-	-	42.0	58	11.7	68.9	92.6
VisualBERT(2019)	592	21.7	32.4	43.9	122	17.9	43.7	65.4
VILBERT(ICLR 2020)	483	23.3	33.5	45.7	131	22.3	55.2	76.1
MKGformer(SIGIR 2022)	221	25.6	36.7	50.4	28	94.4	96.1	97.2
LAFA(AAAI 2024)	<u>136</u>	26.9	39.8	55.1	<u>25</u>	94.7	96.5	97.7
NativE(SIGIR 2024)	149	25.4	38.6	54.2	35	94.2	95.8	97.1
SGMPT*(ACMMM 2024)	238	25.2	37.0	51.0	29	94.3	<u>96.6</u>	97.8
MyGO*(AAAI 2025)	-	19.0	28.9	44.7	-	70.6	93.7	94.1
MPIKGC*(COLING 2024)	-	24.4	35.8	50.3	-	-	-	-
AdaMF-MAT*(COLING 2024)	-	23.1	35.0	49.1	-	73.6	94.3	95.8
Uni-modal KGC Models								
KICGPT (EMNLP 2023)	154	32.7	44.8	55.4	<u>25</u>	93.5	95.6	96.8
MKGL (NeurIPS 2024)	172	32.5	45.4	59.1	31	93.6	95.4	96.3
K-ON (AAAI 2025)	144	33.2	45.7	59.8	26	94.3	95.7	97.2
GLTW (ACL 2025)	-	<u>35.1</u>	<u>48.1</u>	<u>61.4</u>	<u>17</u>	<u>95.2</u>	96.3	<u>97.9</u>
PEKGC (EMNLP 2025)	-	33.6	46.6	54.4	30	94.8	96.0	96.9
ELMM(Ours)	105	37.4	50.2	63.7	11	96.1	97.8	98.9

* indicates that the result comes from SGMPT (Liang et al., 2024).

Table 2: Models performance on the FB15k-237-IMG and WN18-IMG datasets. **Bold** and underline text indicate the best and second-best performance, respectively.

3 Experiments

3.1 Datasets

We evaluate the performance of ELMM on four publicly available multimodal knowledge graph datasets: FB15k-237-IMG (Bollacker et al., 2008), WN18-IMG (Bordes et al., 2013), DB15K(Liu et al., 2019) and MKG-W(Xu et al., 2022). Each dataset comprises three modalities: (1) structured knowledge graph triples, (2) textual descriptions of entities, and (3) a set of associated images per entity. Detailed statistics for both datasets are presented in Table 1. Due to space constraints, we report evaluation results primarily on the FB15k-237-IMG and WN18-IMG datasets in the main text; **results on DB15K and MKG-W are provided in Appendix D**.

3.2 Setting

We adopt LLaVA-1.5 7B (Liu et al., 2024) as the base multimodal large language model (MLLM), incorporating Low-Rank Adaptation (LoRA) (Hu et al., 2022) techniques into both the query and value layers to enable parameter-efficient fine-tuning. The parameter K in the attention pruning strategy is always set to 16, indicating that 16 attention modules in the MLLM are pruned and replaced with linear projections. Full hyperparameter configurations are provided in the Appendix C.

To evaluate the effectiveness of ELMM on the Multimodal Knowledge Graph Completion

(MKG), we adopt standard evaluation metrics, including Hits@k (including Hits@1, Hits@3, and Hits@10) to assess ranking precision at different thresholds, and Mean Rank (MR) to measure the average ranking position of the correct target entities among the predictions.

For a comprehensive performance comparison on FB15k-237-IMG and WN18-IMG datasets, we benchmark our model against two representative categories of methods: (i) multimodal knowledge graph completion methods, and (ii) uni-modal knowledge graph completion methods. The former category includes TransAE (Wang et al., 2019), RSME (Wang et al., 2021), KG-BERT (Yao et al., 2019), VisualBERT (Li et al., 2019), ViLBERT (Su et al., 2019), MKGformer (Chen et al., 2022), LAFA (Shang et al., 2024), NativE (Zhang et al., 2024b), SGMPT (Liang et al., 2024), MyGO (Zhang et al., 2024a), MPIKGC (Xu et al., 2024), and AdaMF-MAT (Zhang et al., 2024c). The LLM-based uni-modal knowledge graph completion baselines include KICGPT (Wei et al., 2024), K-ON (Guo et al., 2025b), GLTW (Luo et al., 2025), PEKGC (Wang et al., 2025) and MKGL (Guo et al., 2024a).

3.3 Comparison with State-of-the-art

We conduct a comprehensive comparison between the proposed ELMM method and 18 state-of-the-art models across FB15k-237-IMG and WN18-

IMG datasets. As shown in Table 2, ELMM consistently outperforms all competing methods across all evaluation metrics. Notably, on the FB15k-237-IMG dataset, ELMM demonstrates substantial improvements over most powerful multimodal approaches, achieving relative gains of 39.0%, 26.1%, and 15.6% in Hits@1, Hits@3, and Hits@10, respectively. These improvements primarily stem from ELMM’s ability to directly leverage the expressive reasoning capabilities of MLLMs to jointly model multimodal information within a unified semantic space. As a result, ELMM more effectively resolves ambiguous cases and entities that require fine-grained visual reasoning. These results strongly demonstrate the potential of MLLMs for MKGC. Furthermore, compared to uni-modal methods based on large language models, ELMM exhibits clear advantages on both datasets, underscoring its effectiveness and robustness in extracting and integrating multimodal information.

3.4 Ablation Study

To evaluate the effectiveness of each component in ELMM, we conduct a series of ablation studies by removing or modifying key modules of the model. Specifically: w/o Image removes the visual views image token representations (I_{image}); w/o Text removes the textual view image token representations (I_{text}); w/o MVTC removes MVTC and does not compress image tokens; w/o pruning indicates the removal of the attention pruning strategy, and MLLM is not pruned; w/o Linear removes the linear compensation mechanism and replaces it with a standard residual connection; w/o Init replaces the initialization strategy of the compensation matrix W_c proposed in Theorem 1 with zero initialization; and head layer replaces the multimodal knowledge reasoning completion layer with a conventional head-layer.

As shown in Table 3, w/o Text performance has declined significantly, while w/o Image has not declined significantly. This indicates that image tokens associated with textual context are more critical in the MKGC task. One possible explanation is that the importance of the same token may vary across different relations (as illustrated in Figure 1), a unique aspect of MKGC that I_{image} representations fail to fully capture. Moreover, removing the MVTC component leads to a substantial performance drop in ELMM, primarily due to increased noise and intensified modality conflicts caused by the large number of image tokens. This

Model	MR	Hits@1	Hits@3	Hits@10
ELMM	<u>105</u>	37.4	50.2	<u>63.7</u>
- w/o Image	115	37.6	49.8	63.1
- w/o Text	146	33.5	46.3	60.7
- w/o MVTC	187	28.5	41.5	56.2
- w/o Pruning	102	37.1	<u>50.0</u>	64.2
- w/o Linear	146	35.9	47.7	60.6
- w/o Init	140	36.8	47.5	61.5
- Head Layer	119	<u>37</u>	49.2	63.0

Table 3: Ablation study results for the FB15k-237-IMG dataset. Bold and underline denote the best and second-best performance of compressed models.

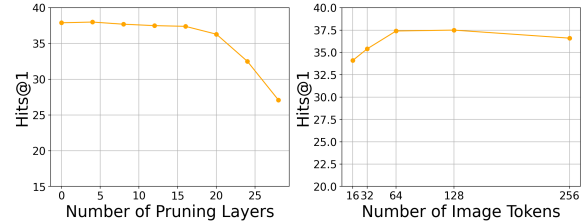


Figure 4: Hyperparameter analysis results. Left: Relationship between Hits@1 and the number of attention pruning layers. Right: Relationship between Hits@1 and number of image tokens are retained after MVTC.

ablation result further confirms that directly applying MLLMs to the MKGC task yields suboptimal outcomes. **It highlights the necessity of designing targeted image token compression and selection mechanisms to mitigate cross-modal information interference specific to this task.**

Notably, ELMM achieves over 30% faster inference without significant performance degradation compared to the non-pruned model, indicating redundancy in attention modules for the MKGC task. Moreover, removing the linear compensation or initializing its projection weights W_c to zero both lead to comparable performance drops, suggesting that the effectiveness of linear compensation depends critically on appropriate initialization. Also, removing the multimodal knowledge reasoning completion layer similarly hurts overall performance.

3.5 Parameter Sensitivity Analysis

3.5.1 Number of Pruning Layers

In our propose attention pruning strategy, we employ a similarity-based criterion to identify and prune the top- K most similar layers. We evaluate the impact of pruning layers on performance, and the corresponding results are shown in Figure 4(left). Experimental findings indicate that the model maintains stable performance when the num-

ber of pruned layers is relatively small, implying a degree of redundancy in the attention modules of multimodal large language models (MLLMs) for MKGC. However, a marked degradation in performance is observed when the pruning depth exceeds 17 layers. Based on this analysis, we fix the pruning depth at 16 layers to achieve a favorable trade-off between inference efficiency and task accuracy.

3.5.2 Number of Image Tokens are Retained After MVTC

We systematically evaluate the impact of the number of retained image tokens on model performance, as shown in Figure 4(right). Overall, performance improves as more image tokens are preserved, indicating the positive contribution of visual information to multimodal knowledge graph completion. However, when the number of retained image tokens exceeds 128, performance degrades, suggesting that excessive visual tokens may introduce redundancy or noise that hampers effective modeling. Balancing predictive performance and computational efficiency, we retain 64 visual tokens in subsequent experiments.

3.6 Impact of Backbone MLLMs on MKGC Performance

To investigate whether ELMM can continuously benefit from the rapid evolution of MLLMs, we study the impact of different backbone models on completion performance. Specifically, we select LLaVA-1.5 7B (Liu et al., 2024), LLaVA-1.5 13B (Liu et al., 2024), and Qwen2.5-VL 7B (Bai et al., 2025) as comparative models. The results are presented in Table 4.

From our experimental results, we observe that while LLaVA-1.5 13B contains a greater number of parameters than LLaVA-1.5 7B, the corresponding performance gains are relatively limited. This outcome may be attributed to the modest difference in parameter count between the two models. In contrast, improvements in the backbone architecture appear to have a more substantial impact on performance. For example, Qwen2.5-VL 7B consistently outperforms LLaVA-1.5 7B and even LLaVA-1.5 13B on several evaluation metrics.

3.7 Inference Time Analysis

We conduct experiments on the FB15k-237-IMG dataset to compare the end-to-end reasoning latency of ELMM with that of state-of-the-art unimodal large language model-based methods, in-

Base Model	MR	Hits@1	Hits@3	Hits@10
LLaVA-1.5 7B	105	37.4	50.2	63.7
LLaVA-1.5 13B	102	37.8	50.7	64.0
Qwen2.5-VL 7B	83	38.6	52.2	64.9

Table 4: Results of ELMM using different base models on the FB15k-237-IMG dataset.

Model Name	Inference Time	MR	Hits@1
ELMM	0.081	105	37.4
MKG	0.126	172	32.5
K-ON	0.084	144	33.2

Table 5: Comparison of ELMM with state-of-the-art uni-modal methods based on large language models in terms of inference time and model performance.

cluding MKGL and K-ON. Specifically, we randomly sample 1,000 instances from the training set for inference, and report the average latency as the inference time. As shown in Table 5, despite the additional cost of processing multimodal inputs, ELMM exhibits lower inference latency than unimodal baselines. This efficiency gain is primarily attributed to the proposed attention pruning strategy, which effectively reduces redundant computation during reasoning. These results demonstrate that ELMM not only outperforms unimodal methods in reasoning efficiency, but also achieves strong performance on standard evaluation metrics by effectively modeling and integrating multimodal information.

4 Conclusion

We propose Efficient Lightweight Multimodal Large Language Models (ELMM), a novel framework that extends MLLMs to the task of MKGC. ELMM addresses two key challenges: (1) semantic noise and modality conflicts caused by excessive image tokens, and (2) the substantial computational overhead associated with processing such inputs using standard MLLMs. To mitigate these issues, we propose a **Multi-view Visual Token Compressor (MVTC)** based on multi-head attention mechanism, which adaptively compresses image tokens from both textual and visual views. We further apply attention pruning to remove redundant attention layers from the MLLMs backbone, improving inference efficiency. To offset any performance degradation from pruning, we add a linear projection with a carefully designed initialization scheme. Experiments on four benchmark datasets, show that ELMM achieves state-of-the-art performance.

Limitations

Although ELMM demonstrates promising effectiveness, it relies on powerful pretrained multimodal backbone models, such as LLaVA and Qwen2.5-VL. While our framework is largely model-agnostic, its performance and efficiency gains are still constrained by the representational capacity of the underlying multimodal large language models (MLLMs).

References

Josh Achiam, Steven Adler, Sandhini Agarwal, Lama Ahmad, Ilge Akkaya, Florencia Leoni Aleman, Diogo Almeida, Janko Altenschmidt, Sam Altman, Shyamal Anadkat, and 1 others. 2023. Gpt-4 technical report. *arXiv preprint arXiv:2303.08774*.

Shuai Bai, Keqin Chen, Xuejing Liu, Jialin Wang, Wenbin Ge, Sibo Song, Kai Dang, Peng Wang, Shijie Wang, Jun Tang, and 1 others. 2025. Qwen2. 5-vl technical report. *arXiv preprint arXiv:2502.13923*.

Kurt Bollacker, Colin Evans, Praveen Paritosh, Tim Sturge, and Jamie Taylor. 2008. Freebase: a collaboratively created graph database for structuring human knowledge. In *Proceedings of the 2008 ACM SIGMOD international conference on Management of data*, pages 1247–1250.

Antoine Bordes, Nicolas Usunier, Alberto Garcia-Duran, Jason Weston, and Oksana Yakhnenko. 2013. Translating embeddings for modeling multi-relational data. *Advances in neural information processing systems*, 26.

Zongsheng Cao, Qianqian Xu, Zhiyong Yang, Yuan He, Xiaochun Cao, and Qingming Huang. 2022. Otkge: Multi-modal knowledge graph embeddings via optimal transport. *Advances in Neural Information Processing Systems*, 35:39090–39102.

Xiang Chen, Ningyu Zhang, Lei Li, Shumin Deng, Chuanqi Tan, Changliang Xu, Fei Huang, Luo Si, and Huajun Chen. 2022. Hybrid transformer with multi-level fusion for multimodal knowledge graph completion. In *Proceedings of the 45th international ACM SIGIR conference on research and development in information retrieval*, pages 904–915.

Yuan Chen, Zichen Wen, Yuzhou Wu, Xuyang Liu, Shuang Chen, Junpeng Ma, Weijia Li, Conghui He, and Linfeng Zhang. 2025. Ipcv: Information-preserving compression for mllm visual encoders. *arXiv preprint arXiv:2512.18747*.

Xiangxiang Chu, Limeng Qiao, Xinyang Lin, Shuang Xu, Yang Yang, Yiming Hu, Fei Wei, Xinyu Zhang, Bo Zhang, Xiaolin Wei, and 1 others. 2023. Mobilevlm: A fast, strong and open vision language assistant for mobile devices. *arXiv preprint arXiv:2312.16886*.

Alexey Dosovitskiy, Lucas Beyer, Alexander Kolesnikov, Dirk Weissenborn, Xiaohua Zhai, Thomas Unterthiner, Mostafa Dehghani, Matthias Minderer, Georg Heigold, Sylvain Gelly, and 1 others. 2020. An image is worth 16x16 words: Transformers for image recognition at scale. *arXiv preprint arXiv:2010.11929*.

Yuxiao Gao, Fuwei Zhang, Zhao Zhang, Xiaoshuang Min, and Fuzhen Zhuang. 2025a. Mixed-curvature multi-modal knowledge graph completion. In *Proceedings of the AAAI Conference on Artificial Intelligence*, volume 39, pages 11699–11707.

Yuxiao Gao, Fuwei Zhang, Zhao Zhang, Xiaoshuang Min, and Fuzhen Zhuang. 2025b. Mixed-curvature multi-modal knowledge graph completion. In *Proceedings of the AAAI Conference on Artificial Intelligence*, volume 39, pages 11699–11707.

Daya Guo, Dejian Yang, Haowei Zhang, Junxiao Song, Ruoyu Zhang, Runxin Xu, Qihao Zhu, Shirong Ma, Peiyi Wang, Xiao Bi, and 1 others. 2025a. Deepseek-r1: Incentivizing reasoning capability in llms via reinforcement learning. *arXiv preprint arXiv:2501.12948*.

Lingbing Guo, Zhongpu Bo, Zhuo Chen, Yichi Zhang, Jiaoyan Chen, Lan Yarong, Mengshu Sun, Zhiqiang Zhang, Yangyifei Luo, Qian Li, and 1 others. 2024a. Mkg1: mastery of a three-word language. *Advances in Neural Information Processing Systems*, 37:140509–140534.

Lingbing Guo, Yichi Zhang, Zhongpu Bo, Zhuo Chen, Mengshu Sun, Zhiqiang Zhang, Wen Zhang, and Huajun Chen. 2025b. K-on: Stacking knowledge on the head layer of large language model. In *Proceedings of the AAAI Conference on Artificial Intelligence*, volume 39, pages 11745–11753.

Qingyu Guo, Fuzhen Zhuang, Chuan Qin, Hengshu Zhu, Xing Xie, Hui Xiong, and Qing He. 2020. A survey on knowledge graph-based recommender systems. *IEEE Transactions on Knowledge and Data Engineering*, 34(8):3549–3568.

Zhiqiang Guo, Jianjun Li, Guohui Li, Chaoyang Wang, Si Shi, and Bin Ruan. 2024b. Lgmrec: Local and global graph learning for multimodal recommendation. In *Proceedings of the AAAI Conference on Artificial Intelligence*, volume 38, pages 8454–8462.

Edward J Hu, Yelong Shen, Phillip Wallis, Zeyuan Allen-Zhu, Yuanzhi Li, Shean Wang, Lu Wang, Weizhu Chen, and 1 others. 2022. Lora: Low-rank adaptation of large language models. *ICLR*, 1(2):3.

Yangqin Jiang, Yuhao Yang, Lianghao Xia, and Chao Huang. 2024. Diffkg: Knowledge graph diffusion model for recommendation. In *Proceedings of the 17th ACM international conference on web search and data mining*, pages 313–321.

Jaejun Lee, Chanyoung Chung, Hochang Lee, Sungho Jo, and Joyce Whang. 2023. *VISTA: Visual-textual*

knowledge graph representation learning. In *Findings of the Association for Computational Linguistics: EMNLP 2023*, pages 7314–7328, Singapore. Association for Computational Linguistics.

Liunian Harold Li, Mark Yatskar, Da Yin, Cho-Jui Hsieh, and Kai-Wei Chang. 2019. Visualbert: A simple and performant baseline for vision and language. *arXiv preprint arXiv:1908.03557*.

Xinhang Li, Xiangyu Zhao, Jiaxing Xu, Yong Zhang, and Chunxiao Xing. 2023. Imf: Interactive multimodal fusion model for link prediction. In *Proceedings of the ACM Web Conference 2023*, pages 2572–2580.

Ke Liang, Lingyuan Meng, Yue Liu, Meng Liu, Wei Wei, Suyuan Liu, Wenxuan Tu, Siwei Wang, Sihang Zhou, and Xinwang Liu. 2024. Simple yet effective: Structure guided pre-trained transformer for multi-modal knowledge graph reasoning. In *Proceedings of the 32nd ACM International Conference on Multimedia*, pages 1554–1563.

Haotian Liu, Chunyuan Li, Yuheng Li, and Yong Jae Lee. 2024. Improved baselines with visual instruction tuning. In *Proceedings of the IEEE/CVF conference on computer vision and pattern recognition*, pages 26296–26306.

Ye Liu, Hui Li, Alberto Garcia-Duran, Mathias Niepert, Daniel Onoro-Rubio, and David S Rosenblum. 2019. Mmkg: multi-modal knowledge graphs. In *The semantic web: 16th international conference, ESWC 2019, portorož, Slovenia, June 2–6, 2019, proceedings 16*, pages 459–474. Springer.

Xinyu Lu, Lifang Wang, Zejun Jiang, Shichang He, and Shizhong Liu. 2022. Mmkrl: A robust embedding approach for multi-modal knowledge graph representation learning. *Applied Intelligence*, pages 1–18.

Kangyang Luo, Yuzhuo Bai, Cheng Gao, Shuzheng Si, Zhu Liu, Yingli Shen, Zhitong Wang, Cunliang Kong, Wenhao Li, Yufei Huang, Ye Tian, Xuantang Xiong, Lei Han, and Maosong Sun. 2025. GLTW: Joint improved graph transformer and LLM via three-word language for knowledge graph completion. In *Findings of the Association for Computational Linguistics: ACL 2025*, pages 11328–11344, Vienna, Austria. Association for Computational Linguistics.

Hatem Mousselly-Sergieh, Teresa Botschen, Iryna Gurevych, and Stefan Roth. 2018. A multimodal translation-based approach for knowledge graph representation learning. In *Proceedings of the Seventh Joint Conference on Lexical and Computational Semantics*, pages 225–234.

Bin Shang, Yinliang Zhao, Jun Liu, and Di Wang. 2024. Lafa: Multimodal knowledge graph completion with link aware fusion and aggregation. In *Proceedings of the AAAI Conference on Artificial Intelligence*, volume 38, pages 8957–8965.

Weijie Su, Xizhou Zhu, Yue Cao, Bin Li, Lewei Lu, Furu Wei, and Jifeng Dai. 2019. Vl-bert: Pre-training of generic visual-linguistic representations. *arXiv preprint arXiv:1908.08530*.

Quan Sun, Yufeng Cui, Xiaosong Zhang, Fan Zhang, Qiyi Yu, Zhengxiong Luo, Yueze Wang, Yongming Rao, Jingjing Liu, Tiejun Huang, and Xinlong Wang. 2024. Generative multimodal models are in-context learners. *Preprint*, arXiv:2312.13286.

Hao Wang, Dandan Song, Zhijing Wu, Yuhang Tian, and Pan Yang. 2025. Path-enhanced pre-trained language model for knowledge graph completion. In *Findings of the Association for Computational Linguistics: EMNLP 2025*, pages 4528–4540, Suzhou, China. Association for Computational Linguistics.

Meng Wang, Sen Wang, Han Yang, Zheng Zhang, Xi Chen, and Guilin Qi. 2021. Is visual context really helpful for knowledge graph? a representation learning perspective. In *Proceedings of the 29th ACM International Conference on Multimedia*, pages 2735–2743.

Xin Wang, Benyuan Meng, Hong Chen, Yuan Meng, Ke Lv, and Wenwu Zhu. 2023. Tiva-kg: A multimodal knowledge graph with text, image, video and audio. In *Proceedings of the 31st ACM International Conference on Multimedia*, MM '23, page 2391–2399, New York, NY, USA. Association for Computing Machinery.

Yu Wang, Nedim Lipka, Ryan A Rossi, Alexa Siu, Ruiyi Zhang, and Tyler Derr. 2024. Knowledge graph prompting for multi-document question answering. In *Proceedings of the AAAI conference on artificial intelligence*, volume 38, pages 19206–19214.

Zikang Wang, Linjing Li, Qiudan Li, and Daniel Zeng. 2019. Multimodal data enhanced representation learning for knowledge graphs. In *2019 International Joint Conference on Neural Networks (IJCNN)*, pages 1–8. IEEE.

Yanbin Wei, Qiushi Huang, James T Kwok, and Yu Zhang. 2024. Kicgpt: Large language model with knowledge in context for knowledge graph completion. *arXiv preprint arXiv:2402.02389*.

Zichen Wen, Yifeng Gao, Shaobo Wang, Junyuan Zhang, Qintong Zhang, Weijia Li, Conghui He, and Linfeng Zhang. 2025. Stop looking for important tokens in multimodal language models: Duplication matters more. *arXiv preprint arXiv:2502.11494*.

Ruobing Xie, Zhiyuan Liu, Huanbo Luan, and Maosong Sun. 2016. Image-embodied knowledge representation learning. *arXiv preprint arXiv:1609.07028*.

Yizhe Xiong, Wei Huang, Xin Ye, Hui Chen, Zijia Lin, Haoran Lian, Zhenpeng Su, Jungong Han, and Guiguang Ding. 2025. Uniatttn: Reducing inference costs via softmax unification for post-training llms. *arXiv preprint arXiv:2502.00439*.

Derong Xu, Tong Xu, Shiwei Wu, Jingbo Zhou, and Enhong Chen. 2022. Relation-enhanced negative sampling for multimodal knowledge graph completion. In *Proceedings of the 30th ACM international conference on multimedia*, pages 3857–3866.

Derong Xu, Ziheng Zhang, Zhenxi Lin, Xian Wu, Zhi-hong Zhu, Tong Xu, Xiangyu Zhao, Yefeng Zheng, and Enhong Chen. 2024. Multi-perspective improvement of knowledge graph completion with large language models. *arXiv preprint arXiv:2403.01972*.

Yantai Yang, Yuhao Wang, Zichen Wen, Luo Zhong-wei, Chang Zou, Zhipeng Zhang, Chuan Wen, and Linfeng Zhang. 2025. **Efficientvla**: Training-free acceleration and compression for vision-language-action models. *Preprint, arXiv:2506.10100*.

Zuoxi Yang. 2020. Biomedical information retrieval incorporating knowledge graph for explainable precision medicine. In *Proceedings of the 43rd International ACM SIGIR Conference on Research and Development in Information Retrieval*, pages 2486–2486.

Liang Yao, Chengsheng Mao, and Yuan Luo. 2019. Kgbert: Bert for knowledge graph completion. *arXiv preprint arXiv:1909.03193*.

Linli Yao, Lei Li, Shuhuai Ren, Lean Wang, Yuanxin Liu, Xu Sun, and Lu Hou. 2024. Deco: Decoupling token compression from semantic abstraction in multimodal large language models. *arXiv preprint arXiv:2405.20985*.

Yichi Zhang, Zhuo Chen, Lingbing Guo, Yajing Xu, Binbin Hu, Ziqi Liu, Huajun Chen, and Wen Zhang. 2024a. Mygo: Discrete modality information as fine-grained tokens for multi-modal knowledge graph completion. *arXiv preprint arXiv:2404.09468*.

Yichi Zhang, Zhuo Chen, Lingbing Guo, Yajing Xu, Binbin Hu, Ziqi Liu, Wen Zhang, and Huajun Chen. 2024b. Native: Multi-modal knowledge graph completion in the wild. In *Proceedings of the 47th international ACM SIGIR conference on research and development in information retrieval*, pages 91–101.

Yichi Zhang, Zhuo Chen, Lei Liang, Huajun Chen, and Wen Zhang. 2024c. Unleashing the power of imbalanced modality information for multi-modal knowledge graph completion. *arXiv preprint arXiv:2402.15444*.

Yichi Zhang and Wen Zhang. 2022. Knowledge graph completion with pre-trained multimodal transformer and twins negative sampling. *arXiv preprint arXiv:2209.07084*.

A License for Scientific Artifacts

The Training dataset FB15k-237-IMG (Bollacker et al., 2008) is licensed under Creative Commons Attribution 4.0 License¹. The Training dataset

¹<https://choosealicense.com/licenses/cc-by-4.0/>

Datasets	MLLM	LoRA r	LoRA dropout	LoRA Target
FB15k-237-IMG	LLaVA-1.5 7B	32	0.05	query, value
WN18-IMG	LLaVA-1.5 7B	32	0.05	query, value
DB15K	LLaVA-1.5 7B	32	0.06	query, value
MKG-W	LLaVA-1.5 7B	32	0.06	query, value

Table 6: LoRA settings in the main experiments.

WN18-IMG (Bordes et al., 2013) is licensed under WordNet Release 3.0 License². The Training dataset DB15K (Liu et al., 2019) is licensed under CC BY-SA 3.0 License³. The Training dataset MKG-W (Xu et al., 2022) is licensed under CC BY-SA 3.0 License⁴. The LLaVA-1.5 model (Liu et al., 2024) and Qwen2.5-VL model (Bai et al., 2025) are licensed under Apache License 2.0⁵. All usages of scientific artifacts in this paper obey the corresponding licenses.

B Related Works

B.1 Multimodal Knowledge Graph Completion

Multimodal knowledge graph completion (MKG) seeks to enhance the reasoning ability of knowledge graphs by jointly leveraging structural triples and multimodal entity information such as images and text. Early approaches (Wang et al., 2019, 2021; Xie et al., 2016) typically used simple feature concatenation, but recent research has introduced more advanced techniques for fine-grained and adaptive multimodal fusion. Representative models include MKGformer (Chen et al., 2022), which employs hybrid transformers with multi-level fusion; SGMPT (Liang et al., 2024) introduces structural information based on MKGformer; LAFA (Shang et al., 2024), which adopts link-aware fusion and neighbor aggregation; MyGO (Zhang et al., 2024a), which tokenizes multimodal entity information for fine-grained representation; and NativE (Zhang et al., 2024b), which addresses modality imbalance in real-world scenarios.

With the rapid advancement of multimodal large language models (MLLMs), these models have demonstrated substantial potential in task related to Multimodal Knowledge Graphs (MKGs). However, most studies have yet to fully explore and exploit the capabilities of MLLMs. To address this gap, we propose ELMM, a novel method designed to harness the strengths of MLLMs.

²<https://wordnetcode.princeton.edu/3.0/README>

³<https://creativecommons.org/licenses/by-sa/3.0/deed.en>

⁴<https://creativecommons.org/licenses/by-sa/3.0/deed.en>

⁵<https://choosealicense.com/licenses/apache-2.0/>

Datasets	Layer of Pruning
FB15k-237-IMG	13,24,28,20,22,29,12,30,9,19,23,21,18,31,5,26
WN18-IMG	27,17,9,20,13,23,30,6,31,14,25,22,21,26,28,19
DB15K	15,27,10,19,17,13,20,29,21,22,31,30,28,23,25,14
MKG-W	19,8,17,16,27,30,23,11,22,29,20,24,21,26,18,31

Table 7: Attention pruning settings in the main experiments.

B.2 Multimodal Large Language Models

With the rapid development of Multimodal Large Language Models (MLLMs), such as GPT-4 (Achiam et al., 2023), LLaVA-1.5 (Liu et al., 2024), Qwen2.5-VL (Bai et al., 2025), and Emu2 (Sun et al., 2024), vision and language understanding have been deeply integrated within a unified semantic space. These models typically adopt a paradigm where visual encoders (Dosovitskiy et al., 2020) segment images into multiple regional patches, which are then encoded into dense image token sequences. These image tokens are projected to align with the dimensionality of text tokens and concatenated with textual inputs for joint processing by transformer backbones, enabling strong performance in visual question answering, image captioning, and general knowledge reasoning tasks.

In recent years, the redundancy of visual tokens has been widely recognized as a major source of increased computational and memory costs in multimodal models, prompting growing interest in addressing the inefficiency caused by excessive image tokens (Yao et al., 2024; Chen et al., 2025; Wen et al., 2025; Yang et al., 2025). For instance, Qwen2.5-VL (Bai et al., 2025) incorporates dynamic resolution adjustment, DeCo (Yao et al., 2024) performs parameter-free adaptive pooling compression at the patch level, and IPCV (Chen et al., 2025) mitigates visual token redundancy through shallow-layer token pruning and neighbor-guided reconstruction for recovering pruned tokens.

However, existing methods compress visual tokens solely based on visual view, which is not well suited for the MKGC task. As demonstrated in Figure 1 and further validated by our ablation studies, **visual tokens that are semantically aligned with the textual modality play a more critical role in MKGC, a factor largely overlooked by prior approaches.** To address this limitation, we propose MVTC, which leverages textual information to identify and preserve the most relevant visual tokens while compressing those that are less infor-

mative. This design facilitates more effective multimodal alignment and fusion in subsequent reasoning stages. Furthermore, to enable the application of MLLMs to MKGC, ELMM proposes several additional innovations beyond MVTC, including an attention pruning strategy and a multimodal knowledge reasoning completion layer. Together, these components allow ELMM to achieve state-of-the-art performance on MKGC benchmarks.

C Further Experiment Details

C.1 Training Hyperparameters.

We adopt LLaVA-1.5 7B (Liu et al., 2024) as the base Multimodal Large Language Model (MLLM), incorporating Low-Rank Adaptation (LoRA) (Hu et al., 2022) techniques into both the query and value layers to enable parameter-efficient fine-tuning. For LoRA related parameter settings, please refer to Table 6. All experiments are conducted using eight NVIDIA A100 GPUs, and both training and inference are implemented with the PyTorch framework. The parameter K in the attention pruning strategy is always set to 16, indicating that 16 attention modules in the MLLM are pruned and replaced with linear projections. To determine which layers to prune, we randomly sample 1,000 training instances and compute the cosine similarity between the attention maps of adjacent layers for each dataset. Layers exhibiting the highest similarity—indicating strong redundancy—are selected for pruning. The specific pruned layers for each dataset are reported in Table 7. The key parameter H in MVTC represents the number of attention headers, and H is set to 32 in all datasets, which represents 32 image tokens each for the textual and visual views, resulting in a total of 64 image tokens. For training parameter settings, please refer to Table 8. We report the version numbers of used packages in Table 9.

C.2 Prompt used in the experiment.

Across all datasets, we employ a unified training and evaluation prompt. Specifically, for instances where the task is to predict the tail entity given a **head** entity and a **relation**, we use the following

Datasets	MLLM	Batch Size	Optimizer	Epoch	Learning Rate
FB15k-237-IMG	LLaVA-1.5 7B	32	Adam	5	3e-4
WN18-IMG	LLaVA-1.5 7B	16	Adam	2	2e-4
DB15K	LLaVA-1.5 7B	64	Adam	2	1e-4
MKG-W	LLaVA-1.5 7B	64	Adam	2	1e-4

Table 8: Training settings in the main experiments.

prompt formulation:

"Next you will be given the Head entity, which has image representations:
<image>.

Suppose that you are an excellent linguist studying a three-word language.
Given the following dictionary:

```
Input\tType\tDescription
{h}\tHead entity\t{h_des}
{r}\tRelation\t{r_des}
```

Please complete the last word (?) of the sentence: {h}{r}?"

Similarly, for instances where the task is to predict the head entity given a **relation** and a **tail** entity, we use the following prompt formulation:

"Next you will be given the Head entity, which has image representations:
<image>.

Suppose that you are an excellent linguist studying a three-word language.

Given the following dictionary:

```
Input\tType\tDescription
{t}\tHead entity\t{t_des}
{inv_r}\tRelation\t{inv_r_des}
```

Please complete the last word (?) of the sentence: {t}{inv_r}?"

Package	Version	Package	Version
PyTorch	2.0.0	transformers	4.48.0
deepspeed	0.10.0	tokenizers	0.20.1
scatter	2.1.2	sparse	0.6.18
datasets	2.14.3		

Table 9: Versions of used packages.

D More Experiment Results.

D.1 Main Results on DB15K and MKG-W.

D.1.1 Comparison Methods and Evaluation Protocol.

Since many methods evaluated on FB15k-237-IMG and WN18-IMG are not tested on DB15K and MKG-W, and vice versa, we re-select the comparison methods to enable a fair and meaningful evaluation on the DB15K and MKG-W

datasets. The selected baselines primarily include IKRL (Xie et al., 2016), TBKGC (Mousselly-Sergieh et al., 2018), TransAE (Wang et al., 2019), MMKRL (Lu et al., 2022), RSME (Wang et al., 2021), VBKGC (Zhang and Zhang, 2022), OTKGE (Cao et al., 2022), IMF (Li et al., 2023), QEB (Wang et al., 2023), VISTA (Lee et al., 2023), AdaMF (Zhang et al., 2024c), MCKGC (Gao et al., 2025b), MyGO (Zhang et al., 2024a), and K-ON (Guo et al., 2025b).

We adopt standard evaluation metrics, including Hits@k (Hits@1, Hits@3, and Hits@10) to measure ranking accuracy at different cutoffs, and Mean Reciprocal Rank (MRR) to evaluate the overall ranking performance of each model.

D.1.2 Main results.

We conduct a comprehensive comparison between the proposed ELMM and 14 state-of-the-art methods on the DB15K and MKG-W datasets. As reported in Table 10, ELMM consistently outperforms all competing approaches across all evaluation metrics, which is in line with the results observed on the FB15k-237-IMG and WN18-IMG datasets. These results demonstrate the robustness and general effectiveness of ELMM for multimodal knowledge graph completion, and further highlight the potential of multimodal large language models (MLLMs) in advancing multimodal knowledge graph completion.

D.2 Robustness Experimental Test.

We conducted a systematic evaluation of the robustness of ELMM under modality-missing scenarios. Specifically, to simulate modality incompleteness in real-world applications, we randomly removed either textual descriptions or visual information from a subset of training samples, while keeping the evaluation procedures unchanged. This setting is designed to assess the ability of ELMM to operate effectively under incomplete multimodal inputs. We considered modality-missing rates of 20%, 40%, 60%, and 80%. For example, a 20% missing rate indicates that 10% of the training samples lack textual information and an additional 10% lack visual information; higher missing rates follow the same proportion.

All experiments were conducted on the FB15k-237-IMG dataset, with Hits@1 adopted as the evaluation metric. The experimental results are illustrated in Figure 5. An interesting phenomenon can be observed: when the modality missing rate is

Model Name	DB15K				MKG-W			
	MRR	Hits@1	Hits@3	Hits@10	MRR	Hits@1	Hits@3	Hits@10
Baseline Models								
IKRL(IJCAI 2017)	26.8	14.1	34.9	49.1	32.4	26.1	34.8	44.1
TBKGC(NAAACL 2018)	28.4	15.6	37.0	49.9	31.5	25.3	34.0	43.2
TransAE(IJCNN 2019)	28.1	21.3	31.2	41.2	30.0	21.2	34.9	44.7
MMKRL(APIN 2025)	26.8	13.9	35.1	49.4	30.1	22.2	34.1	44.7
RSME(MM 2021)	29.8	24.2	32.1	40.3	29.2	23.4	32.0	40.4
VBKGC(KDD 2022)	30.6	19.8	37.2	49.4	30.6	24.9	33.0	40.9
OTKGE(NeurIPS 2022)	23.9	18.5	25.9	34.2	34.4	28.9	36.3	44.9
IMF(WWW 2023)	32.3	24.2	36.0	48.2	34.5	28.8	36.6	45.4
QEB(MM 2023)	28.2	14.8	36.7	51.6	32.4	25.5	35.1	45.3
VISTA(EMNLP 2023)	30.4	22.5	33.6	45.9	32.9	26.1	35.4	45.6
AdaMF(COLING 2024)	32.5	21.3	39.7	51.7	34.3	27.2	37.9	47.2
MyGO(AAAI 2025)	37.7	30.1	41.3	52.2	36.1	29.8	38.5	47.8
MCKGC(AAAI 2025)	<u>39.8</u>	<u>31.9</u>	<u>43.8</u>	<u>54.7</u>	<u>36.9</u>	<u>31.3</u>	<u>38.9</u>	<u>47.4</u>
K-ON (AAAI 2025)	38.1	30.1	42.8	53.6	36.6	30.1	38.7	<u>48.3</u>
ELMM(Ours)	41.2	34.1	45.5	56.7	38.4	33.5	41.7	51.5

Table 10: Models performance on the DB15K and MKG-W datasets. **Bold** and underline text indicate the best and second-best performance, respectively.

set to 20%, the model achieves a noticeable performance improvement compared to the fully observed setting. We hypothesize that a moderate degree of modality missing increases the training difficulty, thereby exerting a regularization effect that encourages the model to learn more robust representations.

As the modality missing rate further increases, the overall Hits@1 performance exhibits a downward trend. Nevertheless, even under relatively high missing rates, the performance degradation remains limited. This observation indicates that ELMM demonstrates strong robustness in modality-missing scenarios. We attribute this robustness to the ability of multimodal large language models to leverage their internal knowledge and contextual reasoning capabilities to partially compensate for missing modality information, thereby mitigating the adverse effects caused by modality incompleteness.

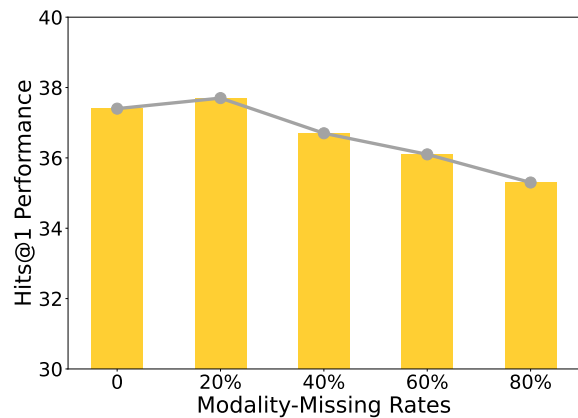


Figure 5: Performance under varying modality-missing rates on FB15k-237-IMG. The y-axis corresponds to Hits@1, and the x-axis represents the proportion of missing modality information.